AGU PUBLICATIONS

Geophysical Research Letters

RESEARCH LETTER
10.1002/2015GL066570

Key Points:
- Stratospheric infrasound is very different from infrasound recorded on ground stations
- Numerous broadband and narrowband signals exist in the stratosphere, some of unknown origin
- Acoustic networks on free floating balloons have unique advantages and disadvantages

Supporting Information:
- Supporting Information S1

Correspondence to:
D. C. Bowman,
daniel.bowman@unc.edu

Citation:
Bowman, D. C., and J. M. Lees (2015), Infrasound in the middle stratosphere measured with a free-flying acoustic array, *Geophys. Res. Lett.*, *42*, 10,010–10,017 doi:10.1002/2015GL066570.

Received 13 OCT 2015
Accepted 28 OCT 2015
Accepted article online 2 NOV 2015
Published online 19 NOV 2015
Corrected 25 JAN 2016
Corrected 14 APR 2016

This article was corrected on 25 JAN 2016 and 14 APR 2016. See the end of the full text for details.

Infrasound in the middle stratosphere measured with a free-flying acoustic array

Daniel C. Bowman[1] and Jonathan M. Lees[1]

[1]Department of Geological Sciences, University of North Carolina at Chapel Hill, Chapel Hill, North Carolina, USA

Abstract Infrasound recorded in the middle stratosphere suggests that the acoustic wavefield above the Earth's surface differs dramatically from the wavefield near the ground. In contrast to nearby surface stations, the balloon-borne infrasound array detected signals from turbulence, nonlinear ocean wave interactions, building ventilation systems, and other sources that have not been identified yet. Infrasound power spectra also bore little resemblance to spectra recorded on the ground at the same time. Thus, sensors on the Earth's surface likely capture a fraction of the true diversity of acoustic waves in the atmosphere. Future studies building upon this experiment may quantify the acoustic energy flux from the surface to the upper atmosphere, extend the capability of the International Monitoring System to detect nuclear explosions, and lay the observational groundwork for a recently proposed mission to detect earthquakes on Venus using free-flying microphones.

1. Introduction

Ground-based infrasound (below audible frequency sound) sensors are a powerful tool for monitoring natural and man-made phenomena that couple with the atmosphere. Infrasound networks can detect volcanic eruptions [*Fee and Matoza*, 2013] and meteors [*de Groot-Hedlin and Hedlin*, 2014], quantify vertical ground motion during earthquakes [*Arrowsmith et al.*, 2012], and track storms in the ocean [*Landès et al.*, 2012]. They are a key component of the International Monitoring System, a global network for detecting nuclear blasts in support of the Comprehensive Test Ban Treaty [*Hedlin et al.*, 2012]. However, acoustic sensors on the Earth's surface suffer from the following shortcomings: (1) they are a quasi two-dimensional observation platform for a three-dimensional phenomenon, (2) the structure of the atmosphere reduces their detection range and may prevent entire classes of signals from being recorded, (3) they are exposed to wind noise, (4) near-sensor topography can distort acoustic signals, and (5) the sensors are subject to ground vibrations.

Despite these drawbacks, few attempts have been made to record infrasound above the surface of the Earth. Arrays on tethered aerostats have been used to quantify the acoustic radiation pattern over simulated volcanic explosions [*Bowman et al.*, 2014] and sonic boom intensity from a prototype high-speed aircraft [*Veggeberg*, 2012; *Naka*, 2012]. Explosion acoustics were investigated using pressure sensors on dropsondes [*Banister and Hereford*, 1991], and signals from a seismic hammer were investigated using microphones on an unmanned aerial vehicle [*Jones et al.*, 2015].

The last infrasound measurements in the stratosphere were made in the early 1960s. The experiment consisted of 30 zero-pressure balloon flights, some reaching up to 22 km altitude. Each balloon payload had one to two pressure sensors that sent data to a ground-based mobile tracking station via a radio link. The sensors detected signals from propeller aircraft and other more enigmatic sources superimposed on an acoustic background originating from turbulence in the troposphere [*Wescott*, 1961a, 1961b, 1964; *Meecham and Wescott*, 1965]. This, along with an Air Force initiative in the 1950s named Project Mogul [*Weaver and McAndrew*, 1995], appears to be the totality of in situ stratospheric infrasound measurements reported in scientific literature prior to the one described here.

We deployed a three-element acoustic array on board a high-altitude balloon to quantify infrasound in the troposphere and stratosphere. The instrumentation maintained an average altitude of 37.5 km above sea level for 5.6 h. Signals recorded on the airborne array consisted of hydrodynamic noise during ascent through the troposphere as well as during the entire descent. Spectral analysis of pressure fluctuations recorded during ascent through the stratosphere and neutral buoyancy consisted of numerous narrowband signals overlain

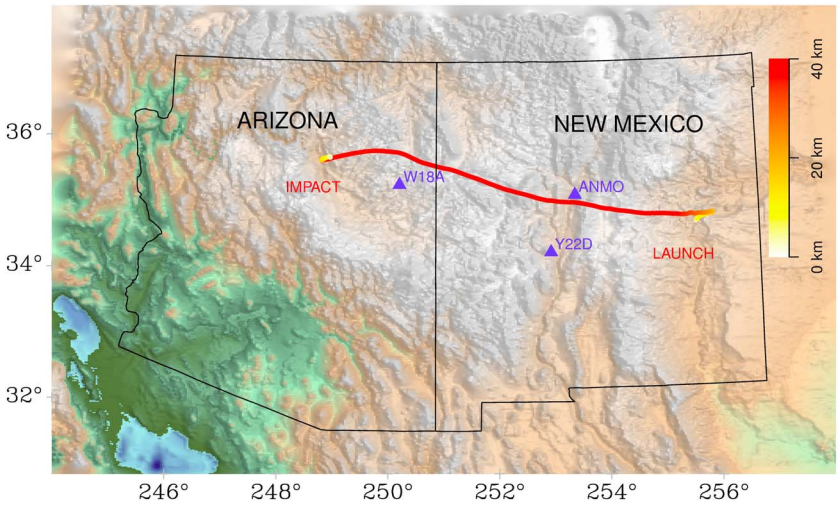

Figure 1. The balloon flight path and permanent ground infrasound stations. The color bar refers to the elevation of the balloon above sea level.

on pulses of broadband activity. Most narrowband signals were not recorded by nearby ground infrasound networks, and the broadband signals did not have clear ground signatures either. While some signals recorded in the air are consistent with acoustic radiation from turbulence, the ocean microbarom, and building ventilation systems, others are more difficult to identify. The novel recording environment and flight system may introduce spurious signals from ambient electromagnetic radiation, the balloon telemetry system, vortex shedding, and cable vibrations; future stratospheric infrasound experiments must be designed with these effects in mind. Our work suggests that the acoustic environment of the stratosphere is dramatically different than that of the ground and that further investigation of this unique region is necessary.

2. Methods

The experiment described here was one of nine payloads on board the High Altitude Student Platform (HASP) [*Guzik et al.*, 2008] that was lifted into the stratosphere using a Winzen 335,000 m^3 zero-pressure balloon. Our infrasound network consisted of three InfraNMT differential pressure transducers [*Marcillo et al.*, 2012]. The sensors were attached to the top, middle, and bottom rungs of the flight ladder that connected the gondola to the balloon envelope; they were named "TOP," "MID," and "BOT," according to their position. The microphone spacing was 6.5 m, creating a vertically oriented linear sensor array with an aperture of 13 m. Data were digitized using an Omnirecs Three-Channel DataCube logger at a sample rate of 400 Hz.

The balloon was launched on 9 August 2014 at 13:25 GMT (7:25 local time) from Fort Sumner, New Mexico, USA. It reached neutral buoyancy at 15:37 GMT and remained at an average altitude of 37,500 m above sea level for the next 5.7 h. The flight was terminated at 21:17 GMT; the sensors landed northeast of Flagstaff, Arizona, USA, at 22:03 GMT (15:03 local time). Three ground infrasound stations were located within 100 km of the flight path (Figure 1); data from these stations were acquired from the International Federation of Digital Seismograph Networks.

The region of pressure fluctuations from the balloon's wake during ascent was quantified via methods outlined in *Barat et al.* [1984]. Temperature and wind speed in the flight region were extracted from the Ground to Space model [*Drob et al.*, 2003]. Ground and balloon sensor range was calculated using the Acoustic Ray Tracer 2-D software package [*Walker et al.*, 2013]. Regions that could transmit sound to the balloon were identified by modeling the free-flying array as an acoustic source via the principle of reciprocity. While the effects of topography on sound propagation can be significant, they were neglected in this case to provide a schematic diagram of the "ideal" sensor range of stratospheric versus ground stations.

Vibrational modes for balloon cabling were calculated via

$$f = \frac{n\sqrt{\frac{T}{\rho}}}{2L} \tag{1}$$

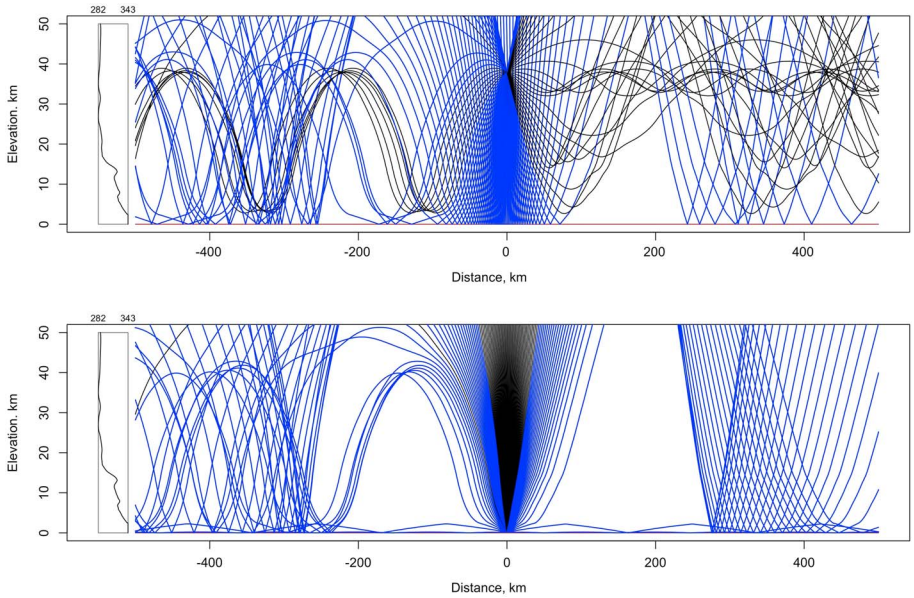

Figure 2. East-west traveling infrasound waves modeled using atmospheric conditions in the balloon's trajectory. (top) The detection range of the microphones during the neutral buoyancy portion of the flight. (bottom) The detection range of a ground station in the same location. Blue rays strike the ground, whereas black rays never reach the surface. View is looking to the south (east negative). The velocity profile for eastward propagating waves is located on the far left of each panel.

where f is frequency, n is the overtone, T is tension, ρ is the mass per unit length of cable, and L is the total length of the cable. Tension on each cable was between 3200 and 4100 N based on the weight of the gondola, ballast, and balloon flight systems. The mass per unit length of steel cable is approximately 0.36 kg/m.

Microphone amplitude response variations due to extreme heat were tested by subjecting them to temperatures of >70°C for several hours in a solar oven. Cold tests were preformed in the same manner in a cooler with dry ice, where temperatures reached −24°C. See supporting information for more discussion on the experimental and analytical methods used in this study.

3. Results

Acoustic propagation modeling suggests that the HASP array sampled a ground region extending approximately 50 km west and 100 km east of the balloon (Figure 2). Sound waves originating between 5 and 38 km elevation could have been detected if they originated east of the balloon. West of the balloon, a narrow wave guide between 35 and 40 km elevation also could have channeled infrasound to the free-flying array. Signals originating at the ground surface more than 200 km away refract off the thermosphere in this case and would have arrived on the HASP array from above. Since sound waves typically refract away from the ground surface in the troposphere, ground stations have a much smaller region over which direct surface arrivals can be detected. The thermospheric duct and eastward extending stratospheric duct are still present, but the elevated wave guide to the west cannot be sampled.

Spectrograms recorded on HASP had different features than those recorded on ground stations (Figure 3 and Figure S2 in the supporting information). The ascent through the troposphere consisted of broadband pressure fluctuations that decreased in amplitude with height (Figure 3). The amplitude of this broadband signal decreased even more dramatically above the tropopause and was absent during the neutral buoyancy portion of the flight. However, it was pervasive during descent, where it did not vary appreciably with altitude.

A series of narrowband signals ranging from approximately 1 Hz to 22 Hz became apparent when the balloon reached the stratosphere. Some of the signals (e.g., between 17 and 22 Hz) do not vary in frequency, whereas others (e.g., some between 10 and 15 Hz) fluctuate by several Hz over a few tens of minutes (Figure 3).

A 17 Hz signal was continuously observed in the stratosphere. A similar spectral peak was also observed on ground station ANMO, which is located about 13 km north of the balloon's trajectory (Figures 1 and S4).

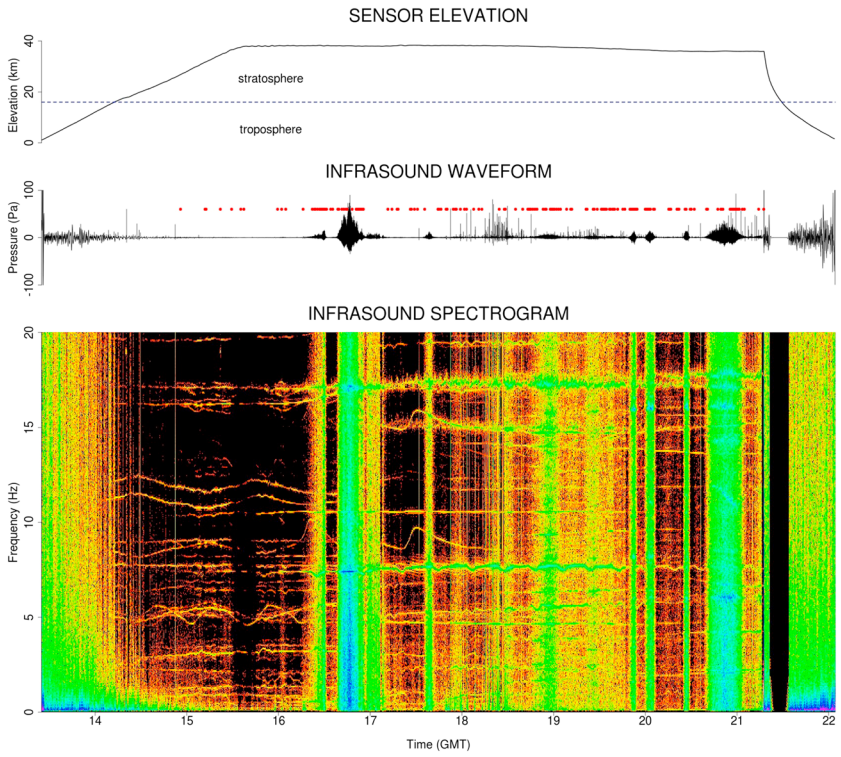

Figure 3. Waveforms and Fourier spectrogram of infrasound signals recorded on the HASP middle sensor. Red dots indicate sections of signal that are statistically indistinguishable from Gaussian noise. An 100 s high-pass filter was applied, and the spectrogram was calculated using a 15 s window with a 14.5 s overlap.

The signal is coherent between HASP and ANMO as the balloon passes by (see Figure S5). The waveforms detected on ANMO originate from the ventilation system of a nearby building. Subsequent indoor infrasound measurements conducted in Pasadena, California, and Chapel Hill, North Carolina, suggest that this 17 Hz pressure fluctuation is common in ventilation systems across the United States.

Episodes of broadband pressure fluctuations begin at about 16:30 GMT and occur throughout the last half of the flight (Figure 3). These pulses of broadband signal can last up to 20 min and have peak-to-peak amplitudes up to 20 Pa in the 0.1–20 Hz range. However, the microphone amplitude response was inconsistent during the flight, and later ground tests indicate that the true amplitudes in the stratosphere are likely higher than those recorded by the sensors.

Sound waves from turbulence in the troposphere were observed in the lower stratosphere during balloon flights in the 1960s [*Wescott*, 1964]. These signals had Gaussian pressure distributions and arrived at an incidence angle of 45° from vertical. We used the Anderson-Darling goodness of fit test to investigate whether the signals we recorded followed a Gaussian distribution also (Figure 3). Time periods where the probability distribution of pressure fluctuations was statistically indistinguishable from the Gaussian distribution seem to occur during the pulses of broadband activity described above. However, broadband signal during ascent and descent were not Gaussian with a confidence of 95%, consistent with the non-Gaussian hydrodynamic noise recorded by *Wescott* [1964] during ascent.

Power spectra of stratospheric infrasound do not resemble those recorded on the ground (Figure 4). Spectra of the three microphones in the stratosphere is concave between 100 s and 1 s, whereas at frequencies above 1 Hz it is convex. In contrast, the power spectra of three ground stations in the flight path have a convex power spectra for the full-frequency range considered. The power levels have a greater range on the ground than they do in the stratosphere, and the spectral peaks seen on the balloon are mostly absent on the ground. Notably, a spectral peak in the microbarom range is present on balloon stations, but not on the ground stations. The ocean microbarom is generated by nonlinear interaction of surface waves in the ocean and can be recorded thousands of kilometers from its source[*Garcés et al.*, 2004]. The spectral power discrepancies

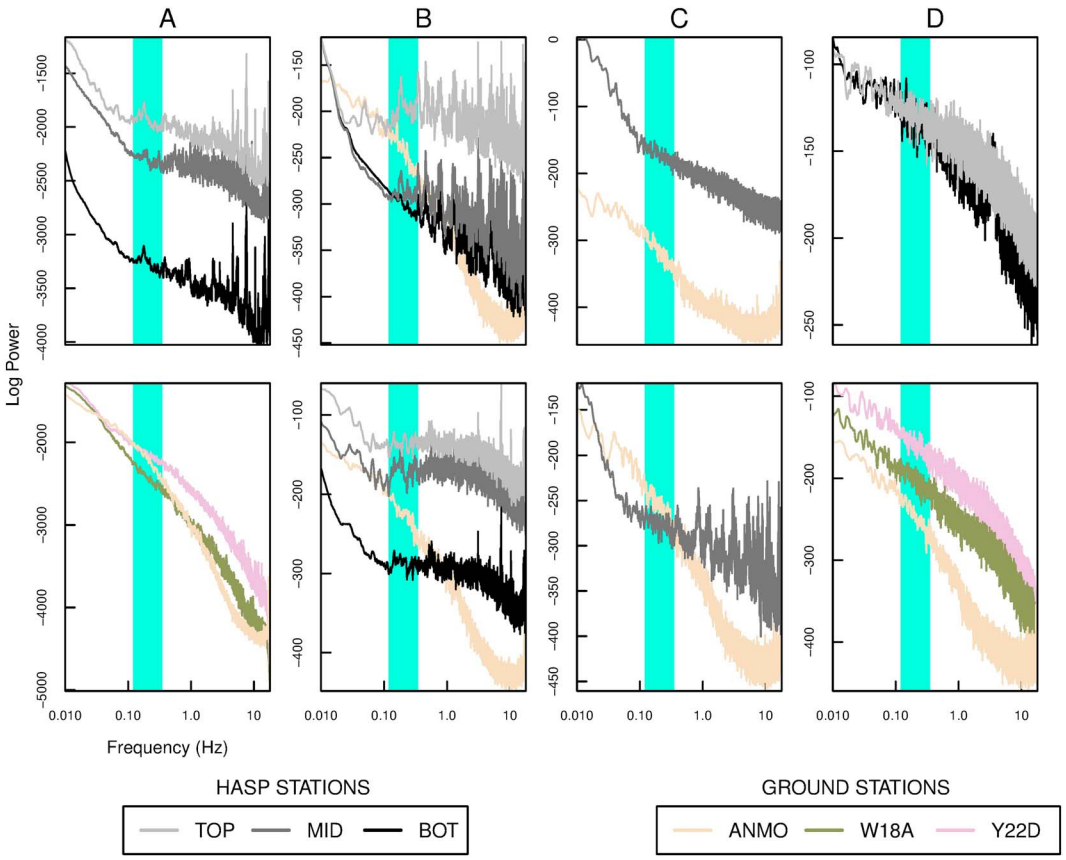

Figure 4. Comparisons of Fourier spectra during different stages of the experiment. (a) Pressure variations (top) during float compared with ground stations (bottom) during the same time period. (b) A period of low-amplitude signals (top) during float (15:38 to 16:15 GMT) compared (bottom) with a period of high-amplitude signals (16:15 to 16:52 GMT) compared with ground station ANMO during the same time periods. (c) Pressure variations during the ascent (top) through the troposphere and the latter portion of ascent (bottom) through the stratosphere compared with ground station ANMO during the same time periods. (d) Spectrum of surviving HASP microphones (top) 1–2 h after landing compared with ground stations (bottom) on the same time interval. The teal box indicates the frequency range of the ocean microbarom [*Campus and Christie*, 2010].

between HASP microphones corresponds to the inconsistent amplitude responses observed during flight. See supporting information for an in-depth discussion of this phenomenon.

Array processing results indicate that the signals arrived nearly perpendicular to the network throughout the flight (see Figure S3) in contrast to those recorded by *Wescott* [1964]. Pressure fluctuations between 10 and 20 Hz appear to arrive slightly below the horizontal plane at times, particularly between 20:30 and 21:00 GMT. In contrast, lower frequency fluctuations appear to arrive horizontally throughout the flight, albeit with much greater scatter.

4. Discussion

The surprising variety of signals recorded on HASP may reflect the greater detection range of stratospheric stations (Figure 2). In addition, propagation modeling indicates that certain regions of the atmosphere are sampled much more effectively with sensors at high elevation (e.g., the narrow wave guide between 35 and 40 km). The ray tracing model presented here neglects topography and does not account for effects such as diffraction, providing a simplified view of the acoustics during the balloon flight. For example, infrasound arrivals can sometimes occur in the regions of silence outlined in Figure 2 due to short-lived wave guides [*Negraru et al.*, 2010] and gravity waves [*Hedlin and Drob*, 2014].

The broadband pressure fluctuations during ascent is consistent with hydrodynamic "wind noise" experienced by infrasound detectors on the ground [*Raspet et al.*, 2006; *Walker and Hedlin*, 2010]. The sensors were

embedded in the balloon's wake as it ascended, creating additional wind noise beyond that contributed by ambient turbulence [*Barat et al.*, 1984]. Pressure amplitudes of hydrodynamic noise can be expressed using Bernoulli's equation for an incompressible fluid:

$$p = \frac{1}{2}\rho u^2 \tag{2}$$

where ρ is fluid density, u is velocity, and p is pressure. Thus, the dramatic decrease in amplitudes observed as the balloon ascended are due to the drop in fluid density (approximately 2 orders of magnitude from the surface to the stratosphere). The lack of pervasive turbulence above the tropopause likely played a role in reducing hydrodynamic noise as well. Such noise was absent during the neutral buoyancy period of the flight because the sensors moved at the same speed as the wind, a marked advantage of balloon-borne networks.

Several mechanisms can explain the narrowband signals recorded during the flight. Wind turbines were visible from the launch facility, and others were located along the balloon's flight path. They are a known generator of narrowband infrasound [*Marcillo et al.*, 2015]. Aircraft can produce a variety of acoustic signals [*Hubbard*, 1991] and are commonly detected by ground infrasound arrays [*Campus and Christie*, 2010]. Piston-engine aircraft signatures with distinct Doppler shifts were observed on balloon-borne infrasound sensors in the 1960s [*Wescott*, 1964]. However, the maximum frequency change of a single narrowband signal during our experiment corresponds to a relative motion of 50 m/s between the sensor and the source [*Lighthill*, 1978], much too slow for commercial aircraft. The acoustic array moved at an average speed of 29 m/s relative to the ground during the neutral buoyancy portion of the flight, so the balloon motion cannot account for these shifts either. This indicates that at least some of the fluctuations we observed are due to changes in source frequency as opposed to relative motions between the emitter and the sensor.

The 17 Hz signal detected on the balloon bears a striking resemblance to infrasound recorded on station ANMO whenever the ventilation system of a nearby building is operating (Figure S4). Since the ventilation system near ANMO is quite small, it is almost certainly not responsible for the totality of the signal recorded on the balloon. Rather, we suggest that the signal recorded in the stratosphere is a "city microbarom" generated by the sum total of ventilation systems in urban areas. While it is localized to inhabited areas on the ground, it may be pervasive in the stratosphere. The lack of observed signal directionality, even when the balloon is close to ANMO (see Figure S3), supports this hypothesis. We speculate that the city microbarom may be a significant means of energy transfer between the Earth's surface and the mesosphere [*Krasnov et al.*, 2007] that did not exist before the widespread use of mechanized air ventilation systems.

Cable vibration may contribute some frequency-invariant narrowband signals. Spectral lines at 8 Hz and 16 Hz between 17:00 and 20:00 GMT could represent a vibrational fundamental mode and first overtone (see Figure 3). Other candidate signals appear between 5 and 6 Hz and 9 and 10 Hz. Vortex shedding from the microphone packages may have occurred during level flight (see supporting information) in which case it may have induced 5 s pressure fluctuations. This could also account for the spectral peak in the microbarom range.

Wescott [1964] reported a quasi-continuous background infrasound signal from turbulence in the troposphere. The pressure fluctuations approximate a Gaussian distribution, as expected from a series of randomly distributed acoustic quadrupoles of various length scales. The episodes of broadband signal recorded during our flight tend to have a Gaussian distribution as well. However, turbulent-driven infrasound reported by *Wescott* [1964] arrived at an incidence angle of 45° from vertical. Based on the lack of time shift across our array, our signals had to have either a nearly horizontal incidence angle, travel much faster than the speed of sound, or consist of something other than plane waves. We propose that infrasound in the stratosphere consists of a diffuse field of pressure waves arriving from multiple directions at once, thus obscuring the arrival angle of individual acoustic sources throughout most of the flight. The balloon was located near the turning point of rays originating in the lower troposphere, perhaps contributing additional simultaneous arrivals across the array. Induction from electromagnetic radiation could cause spurious signals that propagate between the sensors at the speed of light, producing simultaneous arrivals as well. Future high-altitude infrasound investigations should eliminate this possibility by quantifying or preventing induction in signal cabling.

The ocean microbarom is virtually ubiquitous around the globe, but it is often obscured by wind noise [*Christie and Campus*, 2010]. Thus, the presence of the microbarom peak in infrasound spectra provides strong evidence that the network is able to reliably acquire low-amplitude acoustic signals. A spectral peak consistent with the ocean microbarom was recorded during neutral buoyancy flight (Figure 4a), indicating that wind

noise was extremely low during that time. The microbarom peak was absent on ground stations, indicating that wind noise was likely quite high on the Earth's surface. This also may account for the convex shape of the ground station spectra as opposed to the more concave shape of spectra on the high-altitude network.

Power spectra are virtually flat between 10 s and 1 Hz during pulses of broadband activity during the neutral buoyancy portion of the flight, in contrast to quieter periods (Figure 4b). This spectral shape agrees with the Gaussian pressure distributions recorded during the broadband pulses (see Figure 3). In agreement with *Wescott* [1964], we propose that randomly oriented acoustic radiators generated during tropospheric turbulence could account for the observed signals.

Spectra during ascent through the troposphere resemble wind noise dominated spectra on ground stations, whereas spectra from ascent through the stratosphere resemble spectra recorded during the neutral buoyancy part of the flight (Figure 4c, also see Figure 3). Therefore, low-cost-targeted infrasound observations may be feasible in the stratosphere using continuously ascending radiosonde-style balloons.

Upon impact, the two surviving microphones recorded power spectra similar in shape and amplitude to those of ground stations near the balloon's flight path (Figure 4d). This indicates that the spectral differences between ground and stratospheric infrasound reported here reflect distinct acoustic wavefields rather than instrumentation effects.

5. Conclusion

We suggest that acoustic observations on the ground capture a small portion of the infrasound wavefield of the atmosphere. In contrast, free-flying arrays in the stratosphere can resolve signals often obscured by wind noise on the ground (e.g., the ocean microbarom), ones that seldom reach the ground at all (infrasound from turbulence) and ones that refract away from the Earth's surface quickly (air ventilator noise). Quantification of the stratospheric infrasound wavefield may lead to new constraints on the energy flux conveyed by acoustic waves from the lower atmosphere to the thermosphere [*Rind*, 1977; *Hickey et al.*, 2001]. Future balloon-mounted infrasound stations could greatly increase the spatial resolution of the International Monitoring Network by providing low-noise flying stations over regions with no coverage (i.e., the open ocean). Furthermore, free-flying acoustic stations have been proposed as a means of detecting earthquakes on Venus [*Arrowsmith et al.*, 2015]; such a concept could be extended to provide remote detection of atmospheric and surface phenomena on any extraterrestrial body with a significant atmosphere.

Acknowledgments
We thank Doug Drob, Kyle Jones, Omar Marcillo, Rod Whitaker, and Milton Garcés for discussions; T. Gregory Guzik, Michael Stewart, and Doug Granger for making the HASP program possible; Mark Cobble and Jill Juneau for assistance with flight rigging; and Jeff Johnson, Jake Anderson, and Tim Ronan for assistance with instrumentation. This work was supported by National Science Foundation grants DGE-1144081 and CDI-1125185 as well as the University of North Carolina Department of Geological Sciences Martin Fund. Acoustic data will be archived with the Incorporated Research Institutions for Seismology; in the meantime they can be requested from the corresponding author.

References

Arrowsmith, S. J., R. Burlacu, K. Pankow, B. Stump, R. Stead, R. W. Witaker, and C. Hayward (2012), A seismoacoustic study of the 2011 January 3 Circleville earthquake, *Geophys. J. Int.*, *189*, 1148–1158, doi:10.1111/j.1365-246X.2012.05420.x.

Arrowsmith, S. J., D. C. Bowman, L. Rolland, J. M. Lees, D. Mimoun, J. Hall, P. Blom, O. Marcillo, R. W. Whitaker, and G. Nolet (2015), On the use of microbarometers on balloon platforms to probe the internal structure of Venus, *Seismol. Res. Lett.*, *86*(2B), 732–733, doi:10.1785/0220150017.

Banister, J. R., and W. V. Hereford (1991), Observed high-altitude pressure waves from an underground and a surface explosion, *J. Geophys. Res.*, *96*(D3), 5185–5193.

Barat, C., C. Cot, and C. Sidi (1984), On the measurement of the turbulence dissipation rate from rising balloons, *J. Atmos. Oceanic Technol.*, *1*, 270–275.

Bowman, D. C., J. Taddeucci, K. Kim, J. F. Anderson, J. M. Lees, A. Graettinger, I. Sonder, and G. A. Valentine (2014), The acoustic signatures of ground acceleration, gas expansion, and spall fallback in experimental volcanic explosions, *Geophys. Res. Lett.*, *41*, 1916–1922, doi:10.1002/2014GL059324.

Campus, P., and D. R. Christie (2010), Worldwide observations of infrasonic waves, in *Infrasound Monitoring for Atmospheric Studies*, edited by P. Campus and D. R. Christie, pp. 185–234, Springer Sci. and Bus. Media, Netherlands.

Christie, D. R., and P. Campus (2010), The IMS infrasound network: Design and establishment of infrasound stations, in *Infrasound Monitoring for Atmospheric Studies*, edited by D. R. Christie and P. Campus, pp. 29–75, Springer Sci. and Bus. Media, Netherlands.

de Groot-Hedlin, C. D., and M. A. H. Hedlin (2014), Infrasound detection of the Chelyabinsk meteor at the USArray, *Earth Planet. Sci. Lett.*, *402*, 337–345, doi:10.1016/j.epsl.2014.01.031.

Drob, D. P., J. M. Picone, and M. A. Garcés (2003), Global morphology of infrasound propagation, *J. Geophys. Res.*, *108*(D21), 4680, doi:10.1029/2002JD003307.

Fee, D., and R. S. Matoza (2013), An overview of volcano infrasound: From Hawaiian to Plinian, local to global, *J. Volcanol. Geotherm. Res.*, *249*, 123–139, doi:10.1016/j.jvolgeores.2012.09.002.

Garcés, M. A., M. Willis, C. Hetzer, A. Le Pichon, and D. P. Drob (2004), On using ocean swells for continuous infrasonic measurements of wind and temperature in the lower, middle, and upper atmosphere, *Geophys. Res. Lett.*, *31*, L19304, doi:10.1029/2004GL020696.

Guzik, T. G., et al. (2008), Development of the high altitude student platform, *Adv. Space Res.*, *42*, 1704–1714, doi:10.1016/j.asr.2007.04.068.

Hedlin, M. A., and D. P. Drob (2014), Statistical characterization of atmospheric gravity waves by seismoacoustic observations, *J. Geophys. Res. Atmos.*, *119*, 5345–5363, doi:10.1002/2013JD021304.

Hedlin, M. A., K. Walker, D. P. Drob, and C. de Groot-Hedlin (2012), Infrasound: Connecting the solid Earth, oceans, and atmosphere, *Annu. Rev. Earth Planet. Sci.*, *40*, 327–354.

Hickey, M. P., G. Schubert, and R. L. Walterscheid (2001), Acoustic wave heating of the thermosphere, *J. Geophys. Res.*, *106*(A10), 21,543–21,548, doi:10.1029/2001JA000036.
Hubbard, H. H. (Ed.) (1991), *Aeroacoustics of Flight Vehicles: Theory and Practice*, vol. 1, National Aeronautics and Space Administration, Wash.
Jones, K. R., R. E. Abbott, J. Hampshire, R. White, O. Marcillo, and R. W. Whitaker (2015), Infrasound observations from a seismo-acoustic hammer source at the Nevada National Security Site, *Seismol. Res. Lett.*, *86*(2B), 73, doi:10.1785/0220150017.
Krasnov, V. M., Y. V. Drobzheva, and J. Lastovicka (2007), Acoustic energy transfer to the upper atmosphere from sinusoidal sources and a role of nonlinear processes, *J. Atmos. Sol. Terr. Phys.*, *69*, 1357–1365, doi:10.1016/j.jastp.2007.04.011.
Landès, M., L. Ceranna, A. Le Pichon, and R. S. Matoza (2012), Localization of microbarom sources using the IMS infrasound network, *J. Geophys. Res.*, *117*, D06102, doi:10.1029/2011JD016684.
Lighthill, J. (1978), *Waves in Fluids*, Cambridge Univ. Press, Cambridge, U. K.
Marcillo, O., J. B. Johnson, and D. Hart (2012), Implementation, characterization, and evaluation of an inexpensive low-power low-noise infrasound sensor based on a micromachined differential pressure transducer and a mechanical filter, *J. Atmos. Oceanic Technol.*, *29*, 1275–1284, doi:10.1175/JTECH-D-11-00101.1.
Marcillo, O., S. J. Arrowsmith, P. Blom, and K. R. Jones (2015), On infrasound generated by wind farms and its propagation in low-altitude tropospheric waveguides, *J. Geophys. Res. Atmos.*, *120*, 9855–9868, doi:10.1002/2014JD022821.
Meecham, W. C., and J. W. Wescott (1965), High-altitude noise background, in *Proceedings of the 5th International Congress on Acoustics*, vol. 1B, K51 pp., Intl. Commission for Acoustics, Liege, Belgium.
Naka, Y. (2012), *Sonic Boom Data From D-SEND#1, JAXA Research and Development Memorandum*, Japan Aerospace Exploration Agency, Tokyo, Japan.
Negraru, P. T., P. Golden, and E. T. Herrin (2010), Infrasound propagation in the "zone of silence", *Seismol. Res. Lett.*, *81*(4), 615–625, doi:10.1785/gssrl.81.4.615.
Raspet, R., J. Webster, and K. Dillion (2006), Framework for wind noise studies, *J. Acoust. Soc. Am.*, *119*, 834–843, doi:10.1121/1.2146113.
Rind, D. (1977), Heating of the lower thermosphere by the dissipation of acoustic waves, *J. Atmos. Terr. Phys.*, *39*, 445–456, doi:10.1016/0021-9169(77)90152-0.
Veggeberg, K. (2012), Development of a sonic boom measurement system at JAXA, in *Proceedings of the Acoustics 2012 Nantes Conference*, pp. 2017–2022, French Soc. of Acoustics, Nantes, France.
Walker, K. T., and M. A. Hedlin (2010), A review of wind-noise reduction technologies, in *Infrasound Monitoring for Atmospheric Studies*, chap. 5, pp. 141–182, Springer Sci. and Bus. Media, Netherlands.
Walker, K. T., A. Le Pichon, T. S. Kim, C. de Groot-Hedlin, I.-Y. Che, and M. A. Garcés (2013), An analysis of ground shaking and transmission loss from infrasound generated by the 2011 Tohoku earthquake, *J. Geophys. Res. Atmos.*, *118*, 12,831–12,851, doi:10.1002/2013JD020187.
Weaver, R. L., and J. McAndrew (1995), *The Roswell Report: Fact Versus Fiction in the New Mexico Desert*, U.S. Gov. Print. Off., Washington, D. C.
Wescott, J. W. (1961a), High-altitude acoustic research, *J. Acoust. Soc. Am.*, *33*, 847, doi:10.1121/1.1936868.
Wescott, J. W. (1961b), Atmospheric background at high altitudes, in *Proceedings of the Symposium on Atmospheric Acoustic Propagation*, pp. 185–193, Defense Tech. Inf. Center, El Paso, Tex.
Wescott, J. W. (1964), Acoustic detection of high-altitude turbulence, Tech. Rep., The Univ. of Michigan.

Erratum

In the originally published version of this article, a vertical salmon-colored line in all parts of Figure 4 denoted the Brunt-Väisälä (B-V) frequency in radians but the x-axis is in Hz. As a result, the correct B-V frequency in Hz is the current one divided by 2 pi, a value that will be off the scale of the graph. The discussion of the correct value of the B-V frequency is in the Supporting Information file. To correct the inconsistency, the salmon-colored vertical lines have been removed from figure 4, and the mention of the salmon colored line in the caption has been removed. Additionally, the time constant T (tau) was presented in the supplemental information in place of corner period. In section S2, the sentence "TOP had a corner period of 41 $\pm$ 8 seconds, MID had a corner period of 14 $\pm$ 7 seconds, and BOT had a corner period of 38 $\pm$ 4 seconds at the Earth's surface", has been changed to "TOP had a corner period of 250 $\pm$ 48 seconds, MID had a corner period of 85 $\pm$ 32 seconds, and BOT had a corner period of 240 $\pm$ 22 seconds at the the Earth's surface". This version may now be considered the authoritative version of record.